

26 INTRODUCTION

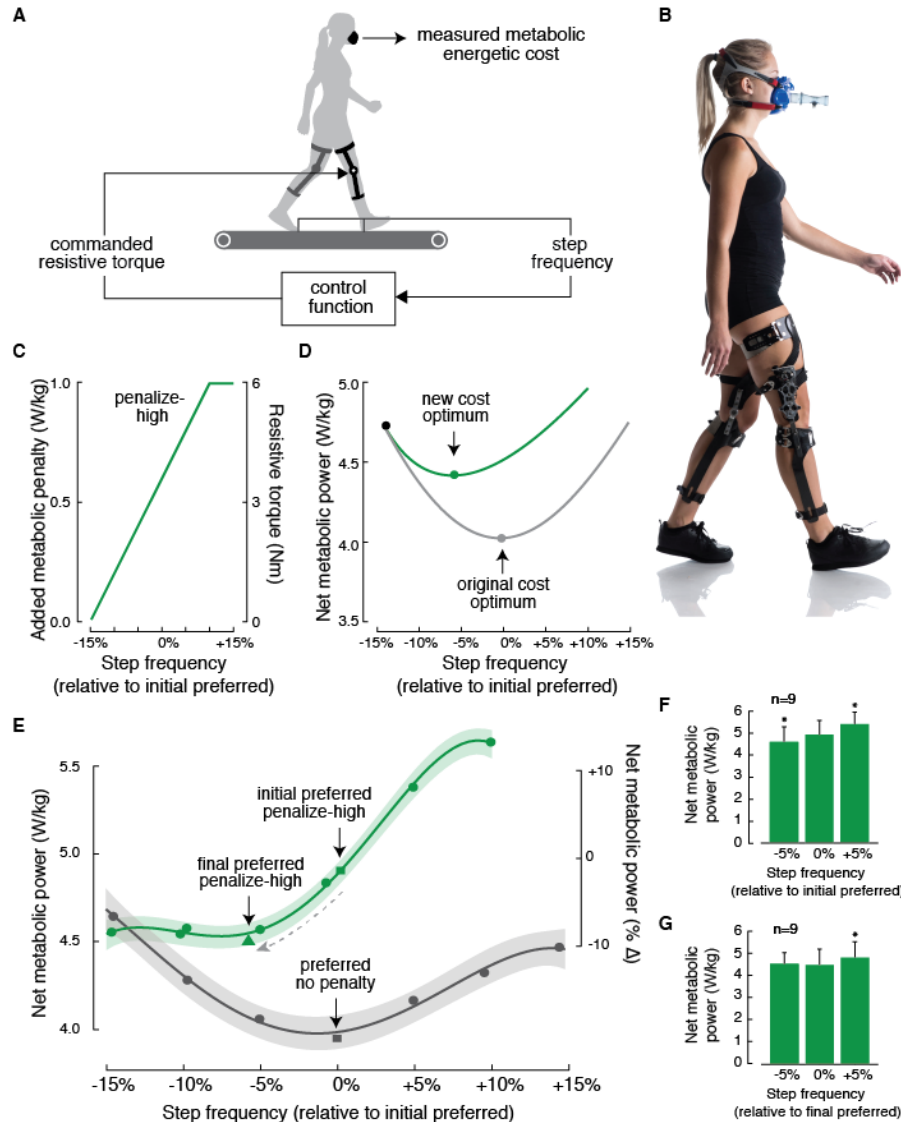
27 People often learn optimal coordination strategies. That is, the nervous system tracks a cost for
28 movement and it adapts its coordination to minimize this cost. This optimization principle
29 underlies theories on the control of reaching, grasping, gaze and gait, although the nervous
30 system may seek to minimize different costs for each of these tasks [1-9]. It has provided insight
31 into healthy and pathological behaviour [10-12], as well as the functions of different brain areas
32 [13]. While there is a growing body of evidence that preferred behaviour in these various tasks
33 indeed optimizes sensible cost functions [1-9,14,15], how the nervous system performs this
34 optimization is largely unknown [2,16].

35 The optimization of movement is a challenge for the nervous system. To perform a movement,
36 the nervous system has thousands of motor units at its disposal, and it can finely vary each motor
37 unit's activity many times per second. This flexibility results in a combinatorially huge number
38 of candidate control strategies for performing most movements—far too many for the nervous
39 system to simply try each one to evaluate its cost [17,18]. The nervous system must instead
40 efficiently search through its options to seek optimal solutions within usefully short periods of
41 time. A second consequence of the large number of control strategies available to the nervous
42 system is that it can never know whether it has truly converged to the best of all possible options.
43 But if it is indeed at an optimum, continuously searching for better options will itself be sub-
44 optimal because all other executed coordination patterns will be more costly [19]. Thus, the
45 nervous system must determine when to initiate optimization and explore new coordination
46 patterns, and when to exploit previously learned strategies [20-22].

47 Here we use human walking to understand how the nervous system initiates and performs the
48 optimization of its motor control strategies. Human walking is a system well suited for studying
49 these questions because the primary contributor to the nervous system's cost—metabolic energy
50 expenditure—is both well established and measurable in this task. Decades of experiments that
51 used respiratory gas analysis have established that our preferred gait parameters—from walking
52 speed [23-26] to step frequency [24,27-29] and step width [30]—minimize energetic cost. While
53 some optimal motor control strategies may be established over relatively long periods of time,
54 we recently discovered that the nervous system can re-optimize aspects of gait within minutes
55 [31]. This is a second reason why human walking is well suited for studying optimization—we
56 can observe energy optimization within a lab setting and within a reasonably short period of
57 time. Studying optimization in tasks such as reaching or saccades is less straightforward as the
58 relevant cost to the nervous system appears to include a term not only for task effort, but also for
59 the task error, and with some unknown weighting between these two contributors [2,5,32,33].
60 Furthermore, motor learning in these tasks appears to, at least initially, prioritize reducing error
61 over optimizing cost, requiring creative experiments to decouple error-based learning from
62 reward-based learning [10,34].

63 To study how the nervous system performs energy optimization in human walking, we leveraged
64 our previously-developed experimental design within which people reliably optimize their gait to
65 minimize energetic cost [31]. In brief, we used lightweight robotic exoskeletons capable of
66 applying resistive torques at the knee joints during walking (**Fig 1**). The exoskeleton controller
67 applies a resistance, and therefore an added energetic penalty, that is minimal at low step
68 frequencies and increases as step frequency increases. Our past experiments demonstrated that
69 this control function reshapes the relationship between step frequency and energetic cost—which

70 we term the *cost landscape*—creating a positively sloped energetic gradient at subjects’ initial
71 preferred step frequency, and an energetic minimum at a lower step frequency. When given
72 sufficient experience with the new cost landscape, subjects in our past experiments learned to
73 decrease their step frequency to converge on the new energetic minimum. We use the term
74 optimization to refer to the process of adapting coordination towards new patterns that minimize
75 cost. This might alternatively be called reward-based adaptation [10,34]. We also distinguish
76 between optimization and prediction, where the former is the process of trying new coordination
77 patterns as the nervous system converges towards the minimum cost, and the latter is the nervous
78 system storing and recalling previously experienced coordination patterns [35,36]. For our
79 purposes we consider prediction, because it involves the storing of a coordination pattern, as
80 commensurate with learning.



81

82 **Fig 1. Experimental design.** (A-B) By controlling a motor attached to the gear train of our
 83 exoskeletons, we can apply a resistance to the limb that is proportional to the subject's step
 84 frequency. (C) Design of the penalize-high (green) control function. (D) Schematic energetic
 85 cost landscapes. Adding the energetic cost of the penalize-high control function to the original
 86 cost landscape (grey) produces a new cost landscape with the optimum shifted to lower step
 87 frequencies (green curve). (E) Measured energetic cost landscapes, reproduced from Selinger et
 88 al. (2015), for the penalize-high (green) control function and controller off condition (grey). The
 89 lines are 4th order polynomial fits, and the shading their 95% confidence intervals, shown only
 90 for illustrative purposes. The dashed grey arrow illustrates the direction of adaptation from initial
 91 preferred (green square) to final preferred step frequencies (green triangle). On average subjects
 92 decreased their step frequency by approximately 6% to converge on the energetic minima and
 93 reduce cost by 8%. (F) The penalize-high control function creates a positively sloped energetic
 94 gradient about the subjects' initial preferred step frequency. (G) Subjects adapted their step
 95 frequency to converge on the energetic minima. Error bars represent 1 standard deviation.

96 Asterisks indicate statistically significant differences in energetic cost when compared to the cost
97 at the initial or final preferred step frequency (0%).

98 Although our prior experiment was the first to provide direct experimental evidence for
99 continuous energy optimization [31], it did not allow us to decipher what experience with a novel
100 cost landscape is critical for optimization to be initiated and what process is used to converge on
101 optima. To understand these mechanisms, here we used a series of experiments that controlled
102 the type of initial experience subjects received with a new energetic cost to determine what gait
103 experience was sufficient for the nervous system to stop exploiting a previously optimal solution
104 and initiate a new optimization. Once the nervous system initiated optimization, we studied how
105 it explored new gaits, in order to understand the nervous system's algorithms for converging on
106 new energetic optima. Using the results of our experiments that examined both the initiation and
107 process of optimization, we then developed computational models based on reinforcement
108 learning that explain how the nervous system may optimize energy during walking.

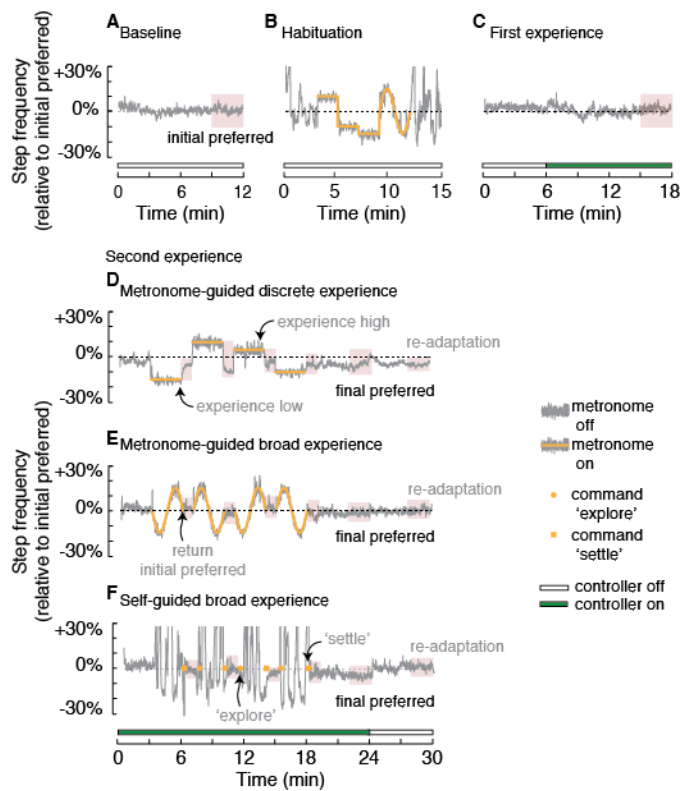
109 **RESULTS**

110 **High natural gait variability may spontaneously initiate optimization**

111 We first sought to determine whether the nervous system could spontaneously initiate
112 optimization and converge on new energetic optima. All subjects first walked for 12 minutes
113 while wearing the exoskeletons, but with the controller turned off (**Fig 2A**, Baseline). This meant
114 that while there was some small inertial and frictional torques from the exoskeleton, there was no
115 additional resistive torque added by the robotic motor [31]. All walking took place on an
116 instrumented treadmill at 1.25m/s and we measured step frequency from treadmill foot contact
117 events [37]. All subjects appeared to settle into a steady state step frequency within 9 minutes

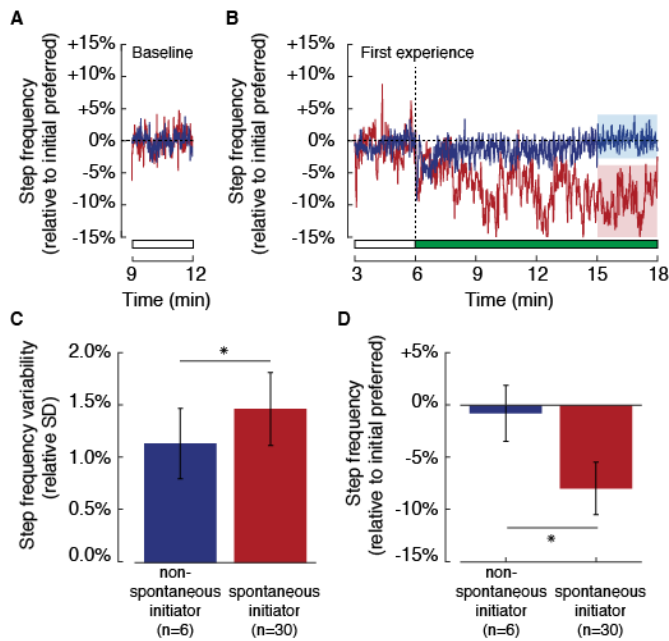
118 and we used the final 3 minutes of walking data to determine subjects' 'initial preferred step
119 frequency'. On average, subjects walked at 1.8 ± 0.1 Hz (mean \pm SD). To guard against the
120 possibility that in future trials subjects could be unaware they are able to alter, or fearful to alter,
121 their step frequency when walking on a treadmill at a constrained speed, we next habituated
122 subjects to walking at a range of step frequencies (**Fig 2B**, Habituation). During this habituation,
123 the controller remained off; therefore, subjects did not gain experience with the new cost
124 landscape. We then turned the controller on, resulting in an applied resistance that was dependent
125 on step frequency, and the subjects walked at a self-selected step frequency for an additional 12
126 minutes (**Fig 2C**, First experience). During this first experience period, 6 of the 36 subjects
127 displayed gradual adaptations in gait and converged to lower, less costly, step frequencies
128 consistent with the energetic optima (**Fig 3A-B**). These subjects, whom we refer to as
129 'spontaneous initiators', had to meet two criteria. First, during the final 3-minutes of the first
130 experience period their average step frequency was required to fall below 3 SD in steady state
131 variability, determined from the final 3-minutes of the baseline period. For most subjects, this
132 equates to a minimum decrease in step frequency of approximately 5%. Second, the change in
133 step frequency could not be an immediate and sustained mechanical response to the exoskeleton
134 turning on. Subjects' final step frequency had to be significantly lower than the step frequency
135 measured in the 10th to 40th second after the exoskeleton turned on (one-tailed t-test, $p < 0.05$).
136 See Supporting Information **Fig S1** for discrimination plot and additional discussion of these
137 criteria. On average, the spontaneous initiators converged toward the optima with an average
138 time constant of 65.7 seconds (exponential fit 95% CI [60.5, 70.8]), or about 120 steps. As
139 determined by our criteria, these *spontaneous initiators* settled on a step frequency that is
140 indistinguishable from the location of the expected optima from our previous experiments [31]

141 (one sample t-test, $t(5)=-0.46$, $p = 0.66$), while the other subjects, or *non-spontaneous initiators*,
142 remained at their initial preferred step frequency (0.8 ± 2.7 %, **Fig 3D**). We hypothesized that
143 high natural gait variability, which results in a more expansive and therefore more clear sampling
144 of the new cost landscape, would be a predicator of spontaneous initiation. To test this, we
145 analyzed individual subjects' step-to-step variability prior to the controller even being turned on
146 and found that spontaneous initiators displayed higher variability in step frequency than non-
147 spontaneous initiators (1.5 ± 0.3 % and 1.1 ± 0.3 %, respectively, two sample t-test, $t(34)=6.06$,
148 $p = 1.8 \times 10^{-2}$, **Fig 3C**). This finding that spontaneous initiation was correlated with higher
149 variability, even before the adaptation itself, was in no way predetermined by our criteria. As a
150 second test of the role of step frequency variability in promoting spontaneous initiation, we
151 regressed the amount of adaptation an individual exhibited during the First Experience period
152 against their step frequency variability from the Baseline period (final 3-minutes), for all 36
153 subjects, and found a weak but significant correlation ($R^2=0.22$, $p = 4.0 \times 10^{-3}$). We expect other
154 factors that vary across individuals, such as the gradient of their cost landscape and their levels
155 of sensory and motor noise, to additionally effect the saliency of the cost landscape, and in turn
156 the likelihood of spontaneous initiation.



157

158 **Fig 2. Experimental protocol.** Each subject completed four testing periods. The first three,
159 Baseline (A), Habituation (B), and First Experience (C), were the same for all subjects. For the
160 Second Experience period, subjects were assigned to either the metronome-guided perturbations
161 to discrete cost points (D), metronome-guided broad experience with the cost landscape (E), or
162 self-guided exploratory experience of the cost landscape (F). Rest periods of 5-10 minutes were
163 provided between each testing period. For all periods, regions of red shading illustrate the time
164 windows during which we assessed steady-state step frequencies. Data shown in A-C and E are
165 from one representative subject, while data in D and F are from two other representative
166 subjects.



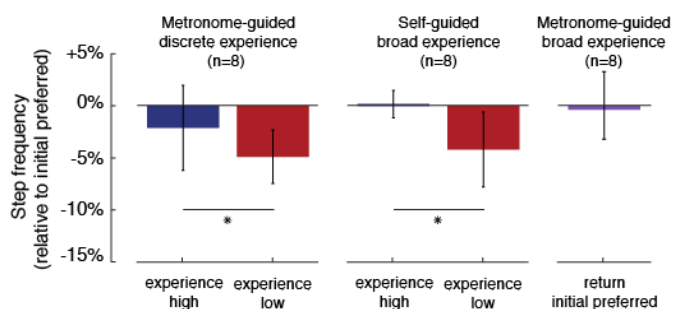
167

168 **Fig 3. Non-spontaneous and spontaneous initiators.** A) Self-selected step frequency during the
169 final 3 minutes of the Baseline testing period for representative non-spontaneous initiator and
170 spontaneous initiator (blue and red, respectively). (B) Step frequency data during the First
171 Experience period for the same two representative subjects. The horizontal bar indicates when
172 the controller is turned on (green fill) and off (white fill). (C) Across all subjects, spontaneous
173 initiators displayed greater average step frequency variability than non-spontaneous initiators
174 during the Baseline testing period. (D) By the final 3 minutes of the First Experience period,
175 spontaneous initiators appeared to adapt their step frequency to converge on the energetic
176 minima, while non-spontaneous initiators did not. Error bars represent 1 standard deviation.
177 Asterisks indicate statistically significant differences for t-tests.

178 Experience with lower cost gaits can initiate optimization

179 We next sought to determine how optimization could be initiated in the non-spontaneous
180 initiators. The non-spontaneous initiators were assigned to one of three experiments (**Table S1**)
181 in which a second experience period included either metronome-guided experience with discrete
182 cost points on a new cost landscape (**Fig 2D**), metronome-guided experience with many costs
183 along a new cost landscape (**Fig 2E**), or self-guided experience with many costs along a new cost
184 landscape (**Fig 2F**). To gain insight into the progress of optimization during this period, 1-minute
185 probes of subjects' self-selected step frequency occurred at the 6th, 10th, and 14th minute, along

186 with a final 6-minute probe at the 18th minute. We found that if, just prior to the first probe,
187 subjects were walking at low step frequencies, and thus experienced lower energetic costs, they
188 appeared to initiate optimization and adapt toward the new optima (**Fig 4**). Yet, if they were
189 walking at high step frequencies, and thus experienced higher energetic cost, they rapidly
190 returned to the initial preferred step frequency (**Fig 4**). This finding was consistent regardless of
191 whether the experience was self-guided (t-test, $t(7)=-2.25$, $p = 0.03$) or metronome-guided (t-test,
192 $t(7)=-2.33$, $p = 0.03$). Moreover, if immediately before the probe subjects were returned to the
193 initial preferred step frequency, as was the case with the metronome-guided experience of many
194 cost points, they showed no adaptation (**Fig 4**; t-test, $t(7)=0.12$, $p = 0.55$). This was despite them
195 having broad experience with the cost landscape. It appears that providing subjects with
196 experience at a low-cost gait and then allowing them to self-select their gait following these new
197 initial conditions is sufficient for initiating optimizing, while expansive experience with the
198 landscape is not. Importantly, the energy cost at the low-cost gait is lower relative to the energy
199 cost at the initially preferred step frequency under the new cost landscape, but not the original
200 cost landscape (**Fig 1E**) indicating that the nervous system is updating its expectation of the
201 energetic consequences of its gaits.

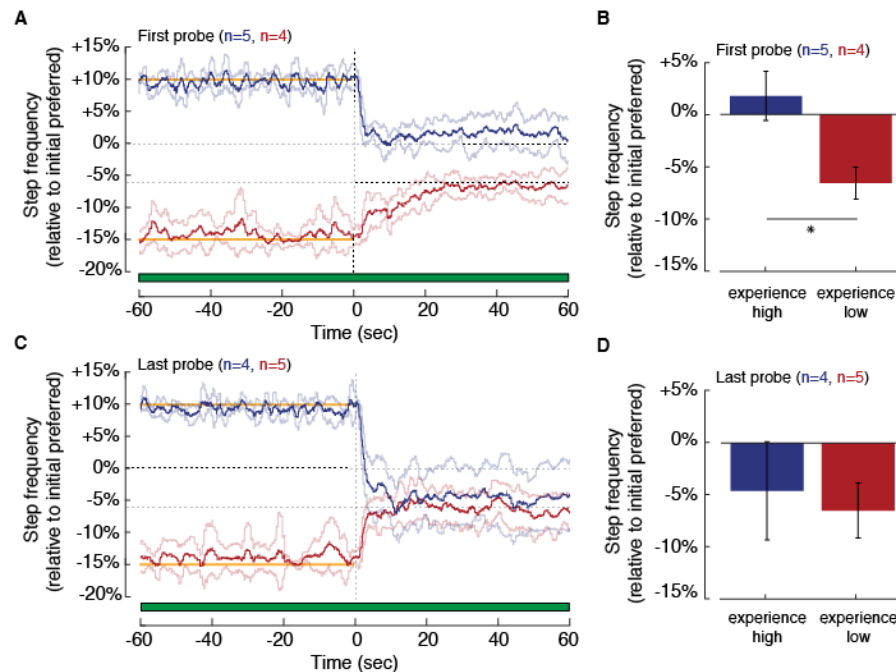


202

203 **Fig 4. Effect of experience direction on initiation of optimization.** For each subject, we
204 averaged data from the final 30 seconds of the first step frequency probe, and then averaged
205 across subjects. Error bars represent 1 standard deviation. Asterisks indicate statistically
206 significant differences for paired t-tests.

207 **A local search strategy is used to converge on energetically optimal gaits**

208 To investigate the interaction between high and low cost experience, as well as the order of the
209 experience, we next compared the behaviour during the first and final probes following
210 experience with the highest (+10%) and lowest (-15%) step frequencies (**Table S1**). We
211 performed a two-way ANOVA and found that both experience direction (high and low cost) and
212 probe order (first and last) had significant effects ($F(1, 17) = 13.25, p = 2.7 \times 10^{-3}$; $F(1, 17) = 4.93,$
213 $p = 0.04$; respectively), as well as their interaction ($F(1, 17) = 5.30, p = 0.04$). A two-sample t-
214 test revealed that step frequencies were significantly different following the first experience with
215 high and low costs ($t(7)=6.1, p = 4.8 \times 10^{-4}$). Following the first experience with high step
216 frequencies subjects appeared to use prediction to rapidly move away from this high cost step
217 frequency (**Fig 5A, Fig S2A**). But, their prediction was erroneous—having not yet experienced
218 lower costs gaits, they returned to their initial preferred step frequency (**Fig 5B, Fig S2A**). They
219 did so with an average time constant of 2.0 seconds (exponential fit 95% CI [1.5 2.5]) or about 4
220 steps. Following the first experience with low step frequencies subjects more slowly descended
221 the cost gradient, with an average time constant of 10.8 seconds (exponential fit 95% CI [9.2
222 12.5]), about 20 steps, and eventually converged on the new optima (**Fig 5A**). Because this was
223 the first probe, all of which followed experience at -15% step frequency, these subjects had no
224 prior explicit experience with the new optima yet could converge to it (**Fig 5B**)—prior explicit
225 experience with the new optima was not necessary for convergence. Subjects' gradual and
226 sequential convergence to the new optima is consistent with a local search process, and
227 inconsistent with alternative optimization methods such as actively sampling from a broad range
228 of new gaits.



229

230 **Fig 5. Effect of experience direction during first and last step frequency probe.** Step
231 frequency time-series data, averaged across subjects, for the first (A) and last (C)
232 following experience either high (blue) or low (red) step frequencies. The light blue and red lines
233 represent 1 standard deviation in step frequency for each time point. The horizontal bars indicate
234 when the controller is turned on (green fill) and off (white fill), and the yellow lines indicate the
235 prescribed metronome frequencies. Steady state step frequencies, averaged across subjects,
236 during the final 30 seconds of the probe for the first (B) and last (D) perturbations toward either
237 high or low. Error bars represent 1 standard deviation. Asterisks indicate statistically significant
238 differences for t-tests.

239 Optimization leads to new predictions of energy optimal gaits

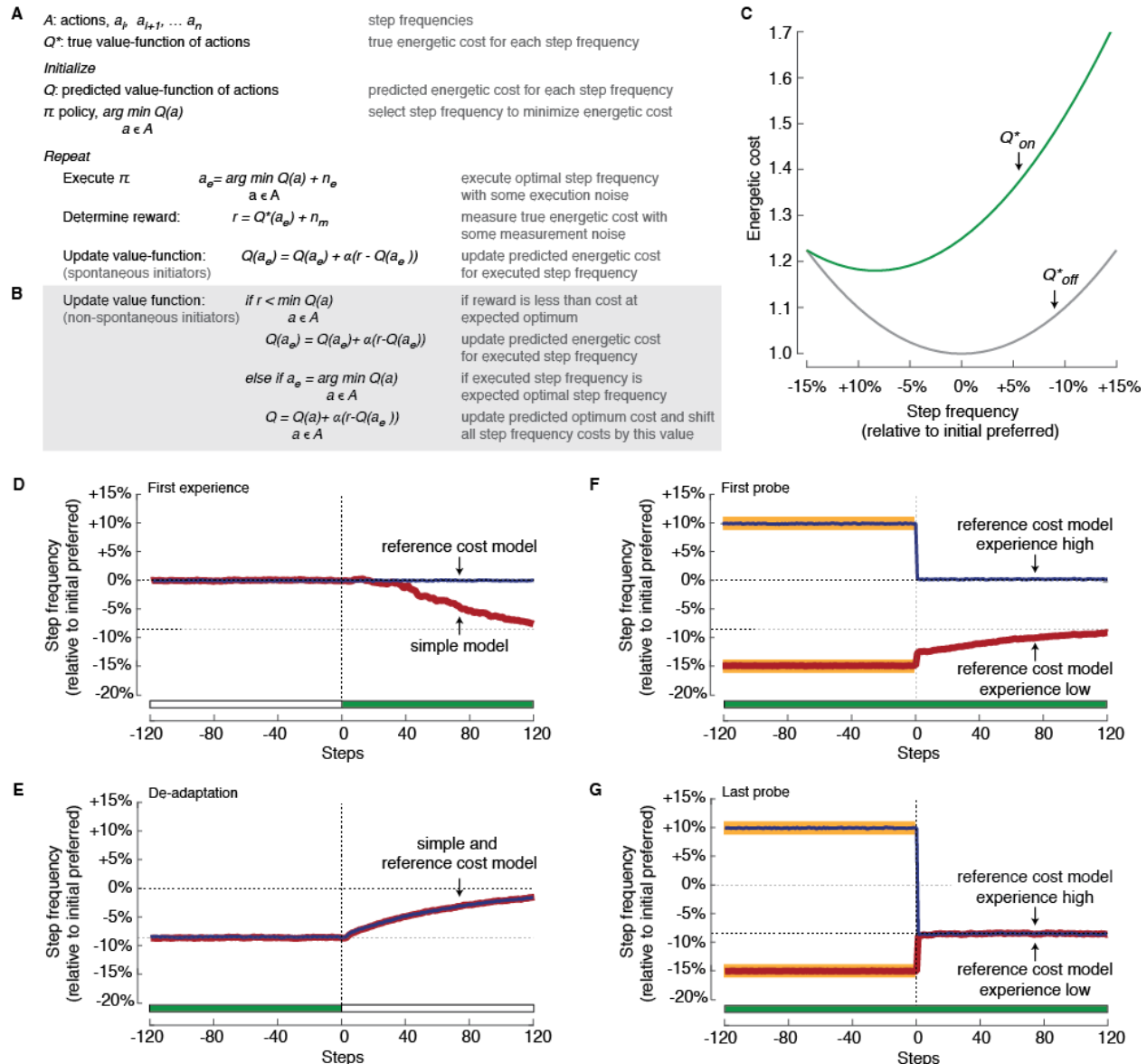
240 During the last probe, subjects rapidly converge on the new optima, with an average time
241 constant of two to three seconds, regardless of the direction of prior experience (experience high:
242 2.8 seconds, exponential fit 95% CI [2.3 3.2]; experience low: 2.5 seconds, exponential fit 95%
243 CI [1.9 3.1]; **Fig 5C-D, Fig S2B**). A two-sample t-test revealed that step frequencies were now
244 indistinguishable following the last experience with high and low costs ($t(7)=0.77, p = 0.47$).
245 Following the last experience at low step frequencies, subjects no longer display slow
246 adaptations consistent with optimization, but instead rapidly predict the optimal gait. And,

247 following the last experience at high step frequencies, subjects' erroneous predictions have been
248 corrected and they rapidly converge to the new cost optimum. This indicates that optimization
249 culminates in the formation of new predictions about optimal movements and the abolishment of
250 old. On average, subjects' 'final preferred step frequency' was -4.8 ± 3.1 %, which was lower
251 than initial preferred (t-test, $t(8)=-4.74$, $p = 1.5 \times 10^{-3}$) and consistent with the expected optima.
252 The high inter-subject variability following the final probe (**Fig 5D**) may in part be due to that
253 fact that each subject will have a different energy optimal step frequencies. When the controller
254 was turned off, returning subjects to the original cost landscape, they slowly unlearned this new
255 prediction. They gradually, with a time constant of 10.5 seconds (exponential fit 95% CI [8.8
256 12.2]), returned to a step frequency indistinguishable from their initial preferred step frequency
257 when the controller was turned off (-0.8 ± 3.0 %).

258 **Energy optimization as reinforcement learning**

259 The experimental behaviours we observed, where in a new environment subjects iteratively learn
260 and then rapidly predict the energy optimal gait, resemble the behaviours produced by classic
261 reinforcement learning algorithms [19,38]. As a proof-of-principle for human motor learning,
262 reinforcement learning algorithms have found the optimal control policies for robots and
263 physics-based simulations that walk, reach, and do other movement tasks [39-41]. And, the
264 necessary components to perform reinforcement learning for human movements, including
265 reward prediction and sensory feedback, are present in our nervous systems and well-studied for
266 learning non-motor tasks [42]. Here we test if a simple reinforcement learning model can indeed
267 reproduce the experimental behaviours observed during energy optimization (**Fig 6A**).
268 Reinforcement learning, applied to our context, allows the nervous system to iteratively learn a

269 *value-function* (Q) that stores the predicted relationship between step frequency and energetic
270 cost. For each new step, the nervous system selects a step frequency, or *action* (a), in accordance
271 with its *policy* (π): ‘choose the energy minimal step frequency’. Each time the nervous system
272 executes a frequency, it measures the resulting energetic cost, or *reward* (r), and updates its
273 predicted cost for that frequency. However, since the reward can’t be measured perfectly due to
274 *measurement noise* (n_m) nor the action executed perfectly due to *execution noise* (n_e), the
275 nervous system doesn’t simply replace the old predicted value with the new reward. Instead it
276 updates the old value by some fraction of the measured reward, referred to as the *learning rate*
277 (α). Our aim here is to demonstrate how a simple reinforcement model of energy optimization
278 can capture the key behavioral features demonstrated by subjects. Our model is not designed to
279 predict or explain individual subjects’ behavior or action histories.



280

281 **Fig 6. Reinforcement learning model of energy optimization.** (A) A simple model describing
 282 the behavior of spontaneously initiating subjects. (B) A more complex logic for updating the
 283 value function that prioritizes learning a reference cost and can describe the behavior of non-
 284 spontaneously initiating subjects. (C) The simulated energetic cost landscapes when the
 285 controller is turned off (Q^*_{off}) and on (Q^*_{on}). Behavior of the simple model of spontaneous
 286 initiators (red) and reference cost model of non-spontaneous initiators (blue) during the First
 287 Experience period when the controller is first turned on (D) and the final de-adaptation period
 288 when the controller is turned off (E). Behavior of the reference cost model of non-spontaneous
 289 initiators during the first (F) and last (G) probes following experience with high (blue) and low
 290 (red) step frequencies. The horizontal bars indicate when the controller is turned on (green fill)
 291 and off (white fill), and the thick yellow lines indicate the prescribed frequencies prior to the
 292 probe.

293 In this model, we specify the following: i) Q^* is initially a representation of the dependence of
294 energetic cost on step frequency during natural walking when the controller is turned off—the
295 original cost landscape (Q^*_{off} , **Fig. 6C**); ii) to simulate the controller turning on, we change Q^* to
296 an accurate representation of the dependence of energetic cost on step frequency under our
297 control function—the new cost landscape (Q^*_{on} , **Fig. 6C**); iii) we represent possible actions as
298 discrete step frequencies; and iv) we set the level of execution noise, measurement noise and
299 learning rate such that the resulting variability in step frequency and rate of convergence to the
300 optimum are comparable to that observed experimentally (See Methods, Model Details).
301 Importantly, the qualitative findings we present below are not particularly sensitive to these
302 specific parameter settings (**Fig S3**).

303 This very simple model can well describe the behaviour of our spontaneous initiators. We find
304 that over about the same number of steps as our human subjects, the model can converge on new
305 energetically optimal gaits to achieve small cost savings (**Fig 6D**). It also learns to predict the
306 new cost landscape, rapidly returning to new cost optima when perturbed away, just as we have
307 found in our human experiments. When returned to the original and previously familiar cost
308 landscape, it doesn't instantly remember old optima but instead has to unlearn its new prediction
309 (**Fig 6E**). Notably, our model does not provide insight into individual subject's behavior, but
310 rather the general behavioural features of energy optimization.

311 This simple reinforcement learner cannot however explain the behaviour of our non-spontaneous
312 initiators. Unlike the majority of our experimental subjects, the above model will always
313 spontaneously initiate optimization and begin converging on the optimal gait (even if the
314 learning rate is adjusted such that past predictions are much more heavily weighted over new
315 measures, **Fig S3A**). Our experimental findings suggest that non-spontaneous initiators may

316 heavily favour exploitation over exploration [19] until sufficient experience with a low-cost gait
317 signals to the nervous system that the current action is suboptimal (See Methods, Model Details).

318 One model that can capture this more complicated behaviour of the nervous system is a
319 reinforcement learner that prioritizes the learning of a reference cost [43-45] that equals the cost
320 at the predicted optimum step frequency (**Fig 6B**). This model continuously relearns the value of
321 the reference cost and then shifts the costs associated with all frequencies by this value. The
322 algorithm only recognizes a change to the shape of the cost landscape when it detects a cost
323 saving with respect to this continuously updated reference cost. It then initiates optimization and
324 updates the cost associated with the individual frequencies that it executes, thereby learning the
325 shape of the new cost landscape. Prioritizing the learning of a reference cost, rather than
326 constantly exploring new gaits, is perhaps a better general strategy for cost optimization in real-
327 world conditions. Energetic cost continuously varies as conditions change in the real world, but
328 unlike our experiment, only some conditions may benefit from the adoption of a new gait and
329 exploring gaits away from the optimal gait comes with an energetic penalty. The continuous
330 updating of a reference cost allows the nervous system to detect when there are reliable costs
331 savings to be gained relative to the predicted optimal gait. It also allows the nervous system to
332 compare differences between the two gaits and understand which walking adjustments led to the
333 lower cost [10,46]. This may allow the nervous system to learn the dimension along which
334 exploration should proceed and quickly converge on the new optimal gait [9,10,47].

335 It is possible that high natural gait variability, as displayed by our spontaneous initiators, is in
336 fact also triggering initiation through the updating of a reference cost because it provides
337 sufficient experience with a low-cost gait. If treated as so, all subjects' behaviour could be

338 explained by the reference cost model. However, deciphering an exact low-cost experience
339 criterion that fits all subject's behaviour, is difficult, and perhaps not possible, as it likely varies
340 across subjects and is affected by additional factors such as the gradient of their cost landscape,
341 their levels of sensory and motor noise, and their weighting of newly experienced costs.

342 This reference cost learning algorithm captures many key behavioral features of our non-
343 spontaneously initiating subjects. First, it does not spontaneously initiate optimization (**Fig 6D**).
344 Second, it only initiates after experience in the new cost landscape with a frequency that has a
345 lower cost than that at the initially preferred frequency. Third, after initiation, the algorithm
346 gradually converges on the new optimum (**Fig 6F**). Finally, much like our original model of
347 spontaneous initiators, after convergence it can leverage prediction to rapidly return to the new
348 optimum after a perturbation (**Fig 6G**) but must slowly unlearn this optimum if returned to the
349 original cost landscape (**Fig 6E**).

350 Overall, our computational models demonstrate that the nervous system may optimize for energy
351 using algorithms consistent with a reinforcement learning framework—leveraging predictions of
352 the optimal gait, and then refining this prediction with the cost of each new walking step. Our
353 experiments and models allow us to describe three key features of energy optimization during
354 gait. First, initiation of optimization appears to be preferentially triggered by experience with low
355 costs gaits, consistent with a prioritization of the learning of a reference cost [43-45]. Second,
356 during optimization the cost of each new walking step results in an updating of the expected cost
357 landscape. And third, this expected cost landscape allows for rapid prediction, and slow
358 unlearning, of energy optimal gaits.

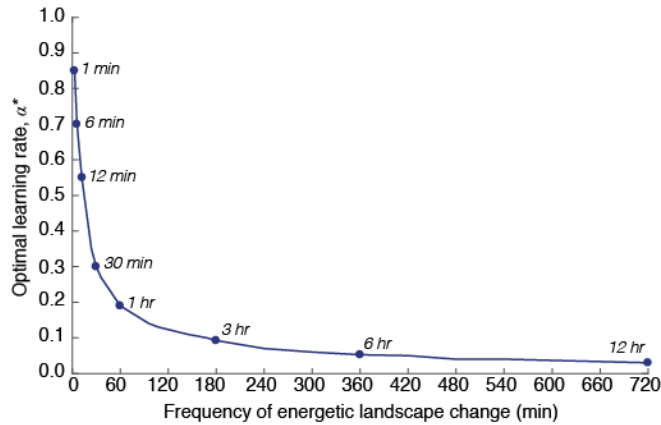
359 **DISCUSSION**

360 Here we used energy minimization in human walking to understand how the nervous system
361 initiates and performs the optimization of its motor control strategies. We found that some
362 people tend to explore, through naturally high gait variability, leading them to spontaneously
363 initiate optimization. Others are more likely to exploit their current prediction of the optimal gait
364 and require experience with lower cost gaits to initiate optimization. When optimization was
365 initiated, people gradually adapted their gait, in a manner consistent with a local search strategy,
366 to converge on the new optima. Given more time and experience, this slow optimization was
367 replaced by a new and rapid prediction of the optimal gait. Our reinforcement learning models
368 reproduce these behaviours, suggesting that the nervous system may use similar mechanisms to
369 optimize gait for energy in walking, and perhaps optimize other movements for other cost
370 functions.

371 Principles of energetic optimality may also determine the nervous system's balance between
372 exploration and exploitation. Variability can aid with initiation by allowing the nervous system
373 to locally sample a more expansive range of the cost landscape, clarify its estimate of the cost
374 gradient, and identify the most promising dimensions along which to optimize [21,48,49]. This
375 variability may simply be a consequence of noisy sensorimotor control that fortuitously benefits
376 the exploration process, or it may reflect intentional motor exploration by the nervous system
377 [21,48]. Recent work suggesting that humans actively reshape the structure of their motor output
378 variability to elicit faster learning of reaching tasks, is evidence of the latter [48]. Learning rate
379 also affects variability because new cost measurements are imperfect. The higher the learning
380 rate, the greater the influence of the new and noisy cost measurements on the predicted optimal

381 movement, resulting in more volatile predictions of the optimal gait and therefore more variable
382 steps. This can speed learning of new optimal strategies in new contexts, reducing the penalty
383 due to the accumulated cost of suboptimal movements during learning. But, there is also a
384 penalty to this high motor variability—once the new optimal strategy is learned, motor
385 variability around this optimum means most movements are suboptimal. The optimal solution to
386 this trade-off depends on how quickly the context is changing (**Fig 7**). It is better to learn quickly
387 and suffer steady state variability about the new optimum when the context is rapidly changing.
388 But, when the context changes infrequently, it is better to learn slowly and more effectively
389 exploit the cost savings at the new optimum. Interestingly, the learning rate in our models, which
390 we chose to match our experimental constraints, is optimal for a cost landscape that is changing
391 approximately every 10-15 minutes, a rate of change not dissimilar from that applied in our
392 experiment protocol. In humans, the nervous system likely has control over the learning rate and
393 the amount of exploration, and may adjust both based on its confidence in the constancy of the
394 energetic conditions. This suggests exploration, and potentially faster learning, could be
395 promoted not through consistent experience in an energetic context, but rather by experimentally
396 alternating energetic contexts.

397



398

399 **Fig 7. Energetically optimal learning rates for varying frequency of cost landscape change.**
400 Measurement and execution noise were set at 2.0% and 1.5%, respectively.

401 Identifying the dimension of an optimization problem may be the trigger for initiation. The
402 coordination of walking is a task of dauntingly high dimension [17,50]. Various gait parameters,
403 including walking speed, step frequency, and step width must be selected, and numerous
404 combinations of muscle activities can be used to satisfy any one desired gait. When presented
405 with new contexts, the nervous system must identify which parameters, if any, to change in order
406 to lower cost. The difficulty of this task may partly explain why non-spontaneous adaptors do
407 not initiate optimization when the exoskeletons are turned on and they are immediately shifted to
408 a higher cost gait. Although it may be clear to the nervous system that costs are higher, it may
409 remain unclear how it should change movement to lower the cost. This could also explain why in
410 some past experiments, by our group [31] and others [27,51], people did not initiate optimization
411 and discover new energy optimal coordination strategies. Experience with lower step
412 frequencies, and therefore lower costs, may allow the nervous system to identify that this is the
413 relevant dimension along which to optimize. This behavioural phenomenon is captured by the
414 addition of a reference cost to our simple reinforcement learning algorithm, and has parallels in
415 classic feedback control models as well as neurophysiological habituation [13,52,53]. Our

416 experiments have demonstrated how the nervous system rapidly solves a one-dimensional
417 optimization problem—where we alter the energetic consequences of a single gait parameter and
418 apply targeted experience along this dimension of gait. How the identified mechanisms extend to
419 optimizing higher dimension movement problems, like those often encountered in real-world
420 conditions, remains an open question for future work.

421 Unveiling the mechanisms that underlie the real-time learning of optimal movements may
422 indicate how this process can be accelerated. This has direct applications in the development of
423 rehabilitation programs, the control of assistive robotic devices, and the design of sport training
424 regimes. A stroke patient faced with a change to their body, a soldier adapting to the new
425 environment created by an exoskeleton, and an athlete attempting to learn a novel task, all seek
426 new optimal coordination strategies. Our findings indicate that eliciting exploration through high
427 motor variability, as well as targeted experience along the relevant movement dimension could
428 rapidly accelerate motor learning in these circumstances by cueing the nervous system to initiate
429 optimization. Therapists and coaches may commonly be doing just this, based on years of
430 accumulated knowledge about effective learning strategies. In this view, a more mechanistic
431 understanding of the nervous system's internal algorithms could aid therapists and coaches in
432 setting a course for a patient or athlete to navigate through various possible movement strategies.

433

434 **METHODS**

435 **Subjects.** Testing was performed on a total of 36 healthy adults (body mass: 63.9 ± 9.8 kg;
436 height: 1.69 ± 0.10 cm; mean \pm SD) with no known gait or cardiopulmonary impairments (Table
437 S1). Simon Fraser University's Office of Research Ethics approved the protocol, and participants
438 gave their written, informed consent before experimentation.

439 Initially, 27 subjects were randomly assigned to one of three experiments (9 subjects per
440 experiments) in which their second experience period included either included either
441 metronome-guided experience with discrete cost points on a new cost landscape (**Fig 2D**),
442 metronome-guided experience with many costs along a new cost landscape (**Fig 2E**), or self-
443 guided experience many costs along a new cost landscape (**Fig 2F**). A preliminary analysis
444 revealed that 5 of the 27 subjects (1 from the metronome-guided discrete experience experiment,
445 1 from the metronome-guided broad experience experiment, and 3 from the self-guided broad
446 experience experiment) appeared to gradually adapt their gait toward the optima during the first
447 experience period, prior to second experience period (**Fig 2C**). These subjects, whom we refer to
448 as 'spontaneous initiators', were therefore not included in the analysis for the second experience
449 periods and were instead analyzed as a separate group. To be considered a spontaneous initiator
450 subjects had to meet two criteria. First, during the final 3-minutes of the first experience period
451 their average step frequency (final step frequency) was required to fall below 3 SD in steady
452 state variability, determined from the final 3-minutes of the baseline period. For most subjects,
453 this equates to a minimum decrease in step frequency of approximately 5%. Second, the decrease
454 in step frequency could not be an immediate and sustained mechanical response to the
455 exoskeleton turning on. The final step frequency had to be significantly lower than the step

456 frequency measured in the 10th to 40th second after the exoskeleton turned on (one-tailed t-test,
457 $p > 0.05$). To rebalance experiments, an additional 2 subjects, both of whom were non-
458 spontaneous initiators, were added to the self-guided broad experience experiment.

459 An analysis of data from the second experience periods indicated that the experience with either
460 high and low step frequencies, and therefore costs, prior to the probe had a lasting effect on the
461 subjects' self-selected step frequency during the probe. To investigate the interaction between
462 high and low cost experience, as well as the order of the experience, we wanted to compare the
463 time course of adaptation during the first and final probes. To achieve the statistical power
464 necessary to do so, we added an additional 7 subjects to the metronome-guided discrete
465 experience experiment. For the added subjects the experience prior to the first or last probes were
466 set to be either the highest (+10%) or lowest (-15%) step frequency, with all other step
467 frequencies assigned in random order. One of the added subjects met the criteria for a
468 spontaneous initiator and was therefore not included in this investigation between experience
469 direction and time. In total for the analysis, 5 subjects experienced +10% and 4 experienced -
470 15% prior to the first probe. Prior to the last probe, 4 subjects experienced +10% and 5
471 experienced -15%. While these subject numbers are low, to detect an across subject average
472 difference in step frequency of at least 5%, given across subject average standard deviation in
473 step frequency of 2.5%, we calculated that we required only 4 subjects per group to achieve a
474 power of 0.8. In addition, we see clear trends in individual subject data (**Fig S2**).

475 In total, 6 of the 36 tested subjects were identified as spontaneous initiators (body mass: $60.8 \pm$
476 10.6 kg; height: 1.68 ± 0.11 cm; mean \pm SD), while 14 were included in the analyses for the
477 metronome-guided discrete experience experiment (body mass: 63.0 ± 10.7 kg; height: $1.69 \pm$

478 0.11 cm; mean \pm SD), 8 for the metronome-guided broad experience experiment (body mass:
479 67.7 ± 9.1 kg; height: 1.71 ± 0.09 cm; mean \pm SD), and 8 for the self-guided broad experience
480 experiment (body mass: 64.2 ± 8.6 kg; height: 1.67 ± 0.07 cm; mean \pm SD).

481 **Detailed Experimental Protocol.** Each subject completed one testing session, lasting three
482 hours with no more than two and half hours of walking to reduce fatigue effects. All subjects
483 experienced the penalize-high control function, which has previously been shown to shift
484 energetic optima to low step frequencies [31] (Fig 1C-G). Subjects were given between 5-10
485 minutes of rest in between each of the walking periods, including baseline, habituation, first
486 experience, and one of the three assigned second experience periods (Fig 2A-F respectively,
487 described in detail below).

488 At the beginning of testing, we instrumented subjects with the exoskeletons and indirect
489 calorimetry equipment (VMax Encore Metabolic Cart, VIASYS®). We then determined their
490 resting energetic cost during a 6-minute quiet standing period. Following this, during the
491 baseline period (Fig 2A), subjects were simply instructed to walk for 12-minutes.

492 Next, subjects completed a habituation period where they were familiarized with walking at a
493 range of step frequencies (Fig 2B). This trial was included to reduce the possibility that in future
494 trials subjects could be unaware they are able to alter, or fearful to alter, their step frequency
495 when walking on a treadmill at a constrained speed (Fig 2B). During this habituation, the
496 controller remained off; therefore, subjects did not gain experience with the new energetic
497 landscape. We explained to the subjects that for a given walking speed it is possible to walk in a
498 variety of different ways, including with very long slow steps or very short fast steps. They were
499 encouraged to explore these different ways of walking during the habituation period. They were

500 also informed that at times a metronome would play different steady state tempos, or slowly
501 changing tempos, and that they should do their best to match their steps to the tempos. During
502 the habituation period, three different steady state tempos were played for three minutes each.
503 These tempos included +10%, -10%, and -15% of the initial preferred step frequency. The
504 sinusoidally varying metronome tempo had a range of $\pm 15\%$ of the initial preferred step
505 frequency and a period of 3 minutes.

506 Prior to the first experience period, we explained to subjects that they would next walk for 6
507 minutes with the exoskeleton turned off, at which point the exoskeleton would turn on and they
508 would walk for a remaining 12 minutes (**Fig 2C**). They were given no other directives about how
509 to walk and at no point during testing were subjects provided with any information about how
510 the controller functioned, or how step frequency influenced the resistance applied to the limb.

511 For the second experience period, subjects completed one of the three experiments: metronome-
512 guided experience with discrete cost points on a new cost landscape (**Fig 2D**), metronome-
513 guided experience with many costs along a new cost landscape (**Fig 2E**), or self-guided
514 experience many costs along a new cost landscape (**Fig 2F**). All subjects were informed that they
515 would be walking for 30 minutes and that the exoskeleton would be on for the first 24 minutes
516 and off for the final 6 minutes. To gain insight into the progress of optimization under each
517 experiment, 1-minute probes of subjects' self-selected step frequency occurred at the 6th, 10th,
518 and 14th minute, along with a final 6-minute probe at the 18th minute (**Fig 2D-F**).

519 Those assigned to the metronome-guided discrete experience experiment were informed that at
520 times the metronome would be turned on, during which they should match their steps to the
521 steady-state tempo, and that when the metronome turned off, they no longer had to remain at that

522 tempo (**Fig 2D**). Besides these instructions, subjects were given no further directives about how
523 to walk. The metronome was turned off at four different time points, each serving as a probe of
524 subjects self-selected step frequency. Prior to each probe, different metronome tempos were
525 played, including -15%, -10%, +5% and +10% of initial preferred step frequency. We chose
526 these tempos such that they spanned the energetic landscape but did not include step frequencies
527 explicitly at the expected optima or the preferred step frequency (approximately -5% and 0%,
528 respectively). Order of the tempos was randomized. The exception to this was that for the 7
529 subjects added to this experiment, either the first or last tempo was randomly assigned as either
530 +10% or -15%, with the remaining 3 step frequencies assigned in random order.

531 Those assigned to the metronome-guided broad experience experiment were given the same
532 instructions as those in the metronome-guided discrete experience experiment, except that they
533 were informed that the metronome tempo would change slowly over time (**Fig 2E**). A
534 sinusoidally varying metronome tempo was played for 3 minutes, 4 separate times, which were
535 once again separated by probes of self-selected step frequency. The sinusoidal tempo had a range
536 of $\pm 15\%$ of the initial preferred step frequency, a period of 3 minutes, and began and therefore
537 ended at 0% of the initial preferred step frequency. These subjects were therefore guided through
538 the complete landscape but always returned to their preferred gait prior to a probe.

539 Those assigned to the self-guided broad experience experiment were informed that at times the
540 experimenter would verbally give them the command 'explore', at which point they should
541 explore walking at a range of different step frequencies (**Fig 2E**). They were informed that they
542 should continue to do so until given the command 'settle', at which point that should settle into a
543 steady step frequency. They were given no directives about what their steady state step

544 frequency should be. Subjects were instructed to explore four separate times, each lasting three
545 minutes and once again separated by probes of self-selected step frequency. When the command
546 settle was given subjects could be at any self-selected step frequency, therefore the experience
547 direction, at high or low cost, was not predetermined.

548 **Experimental Outcome Measures.** Each subject's initial preferred step frequency was
549 calculated as the average step frequency during the final 3 minutes of the baseline period.
550 Individual subject's variability in step frequency, calculated as a coefficient of variation, was
551 also assessed during this time period. Similarly, the average step frequency was calculated
552 during the final 3 minutes of the first experience period. During this period, the spontaneous
553 initiators were found to adapt toward the optima. To determine the average rate at which they did
554 so, step frequency time series data from the 6th to the 18th minute for the subjects was grouped
555 together and fit with a single term time-delayed exponential. Prior to fitting, data was down-
556 sampled to a step rate of 1.8Hz, so as not to overestimate data points and inflate calculated
557 confidence intervals. We used one-tailed t-tests with a significance level of 0.05 to compare the
558 step frequency, as well as variability in step frequency, of the spontaneous and non-spontaneous
559 initiators (**Fig 3C-D**). We used one-tailed t-tests because we expected the spontaneous initiators
560 to present with lower steady-state step frequencies and higher variability.

561 During the second experience periods, 1-minute probes of subjects' self-selected step frequency
562 occurred at the 6th, 10th, and 14th minute, along with a final 6-minute probe at the 18th minute.
563 When statistical comparisons were made between first and last probes following high and low
564 experience, data from the 30th to the 60th second of each of the self-selected step frequency
565 probes were used for analysis. We used t-tests with a significance level of 0.05 (**Fig 4, Fig 5B**

566 and **Fig 5D**). When investigating the rate at which subjects adapted their step frequency, step
567 frequency time series data from the first 60 seconds of the probes from subjects of the same
568 experiment were once again fit with a single term time-delayed exponential, using the same
569 process steps as previously described. For plotting purposes, we averaged across subjects of the
570 same experiment and calculated the across subject standard deviation at each time point.

571 Because there was no effect of experience direction during the last probe, subjects from the high
572 and low experience were grouped. The final preferred step frequency was calculated as the
573 average step frequency during the 21st to 24th minute of the second experience period, just prior
574 to the controller being turned off. The re-adaptation step frequency was calculated as the average
575 step frequency during the final 3 minutes of the second experience period, when the controller
576 was turned off. When investigating the rate at which subjects re-adapted their step frequency
577 back to the initial preferred, step frequency time series data from the entire re-adaptation period
578 were once again fit with a single term time-delayed exponential and the average and standard
579 deviation profiles were calculated for plotting purposes.

580 **Model Details.** The range of possible actions ($a_i, a_{i+1}, \dots a_n$) were set to be discrete integer step
581 frequencies, ranging between -15% and +15%. The simulated energetic cost landscape (Q^*),
582 before the controller was turned on, was modelled as a quadratic function of the form:

$$583 \quad Q^*_{off}(a_i) = 10 \times (a_i/100)^2 + 1,$$

584 having a normalized cost of 1 at the optimum and a curvature that well approximates our
585 experimentally measured landscape. After the controller was turned on, the simulated landscape
586 was modelled as:

587 $Q^*_{on}(a_i) = Q^*_{off}(a_i) + (a_i/60 + 1/4),$

588 where the cost added to $Q^*_{off}(a_i)$ well approximates the energetic effect of our controller, again
589 creating a landscape similar in shape to that which we measure experimentally.

590 The parameters that describe the behavior of the reinforcement learner include: the standard
591 deviation in step frequency execution noise (n_e), the standard deviation in energetic cost
592 measurement noise (n_m), and the weighting parameter, or learning rate (α). On any given step,
593 the levels of measurement and execution noise are drawn from a Gaussian distribution with mean
594 zero and standard deviation determined from the value of the parameter.

595 We performed a sensitivity analysis to determine feasible parameter ranges that are consistent
596 with experimentally measured rates of convergence to the optimum and variability in step
597 frequency. Similar to the design of our experimental first experience period, we simulated a
598 protocol that lasts 1440 steps (approximately 12 minutes) in which the landscape changed from
599 Q^*_{off} to Q^*_{on} after 720 steps (approximately 6 minutes). Using our simple reinforcement leaning
600 model that spontaneously initiates optimization, we varied the execution noise (between 1 and
601 3% of the initial preferred step frequency), measurement noise (between 0.1 and 6% of the
602 energetic cost at the initial preferred step frequency during natural walking), and learning rate
603 (between 0.01 and 1). Model simulations were repeated 1000 times for each possible
604 combination of parameter settings.

605 We then determined the resulting rates of convergence to the optimum by averaging step
606 frequency data across repeats and then fitting the final 720 steps with a single process
607 exponential model. As expected, higher learning rates, which put greater weight on new

608 measurements as opposed to past measurements, lead to faster convergence to the optimum (**Fig**
609 **S3A**). This rate of convergence is largely unaffected by measurement noise, and is only
610 minimally affected by execution noise, where higher execution noise can slow convergence to
611 the optimum. In our experiments, the convergence to the optimum typically occurred with a time
612 constant of less than 100 steps. This experimental constraint leaves us with a wide range of
613 possible learning rate parameter settings, from 0.5-1.0 for any simulated combination of
614 measurement and execution noise. For the purposes of our simulations, we set the learning rate
615 to be 0.5.

616 Given our chosen learning rate, we next selected measurement and execution noise levels that
617 generated variability in step frequency that well approximated that which we observed
618 experimentally during steady state behavior (1.0-1.5%). For each simulation repeat, we
619 calculated the standard deviation in step frequency during the first 720 steps. During this time,
620 the learner is at the Q^*_{off} optimum and the landscape is unchanging, leading to steady state
621 behavior. We then averaged this value across repeats to get an average measure of variability in
622 steady state step frequency for each possible combination of measurement noise and execution
623 noise. Once again, our experimental constraints left us with a wide range of possible parameter
624 settings (**Fig S3B**). For the purposes of our simulations, we set the measurement noise to be
625 2.0% and the execution noise to be 1.5%. Importantly, within the ranges deemed reasonable by
626 our experimental constraints, the qualitative behaviours generated by our model are not
627 particularly sensitive to the specific learning rate, measurement noise, and execution noise
628 parameter settings we chose.

629 Our reference cost model only initiates optimization after sufficient experience with a lower cost
630 gait. It is unclear from our experiments exactly what constitutes sufficient experience with a low-
631 cost gait. For example, it may require a substantially lower cost, a sufficient number of steps at a
632 lower cost, or some combination of these criteria. For the purposes of modelling, we assume that
633 the criteria have been met during the experience with low cost prior to the first probe, in keeping
634 with our experimental findings.

635 Principles of energetic optimality may also determine the choice of learning rate. It is possible to
636 solve for a learning rate that minimizes energy expenditure; however, the optimal learning rate is
637 dependent on how frequently the energetic landscape is changing. To demonstrate this, we
638 simulated protocols where the landscape changes from Q^*_{off} to Q^*_{on} with a period varying
639 between 1 minute and 12 hours, at a duty cycle of 50%. We simulated 24 hours of walking and
640 evaluated learning rates ranging between (between 0.01 and 1). Model simulations were repeated
641 100 times for each possible combination of parameter settings. We then determined the average
642 energetic cost across all steps (before measurement noise was applied), and then averaged across
643 repeats to get an average energetic cost for each combination of period and learning rate. Next,
644 we solved for the learning rate that minimized energetic cost for each period (**Fig 7**).

645 **Alternative Models.** Although our reinforcement learning model is quite simple in form, it is
646 reasonable to ask if even simpler algorithms could capture our experimental behaviour. We first
647 considered models that lacked two key features of our final model—the storing of the entire
648 value function and the need to update a reference cost prior to initiation of optimization.

649 A simplified model that forgoes the storing of the entire value function can reproduce the key
650 features of our experimental data. This simplified no-value function model only stores the

651 optimal gait and its associated cost, rather than the costs at all experienced gaits (i.e. the value
652 function). Yet, it can initiate optimization after experience with a lower cost, converge on a new
653 energetic optimum using a local search, and learn to rapidly predict this optimum when
654 perturbed away. Despite this, we prefer the slightly more complex value-function model because
655 we suspect it will better generalize to learning in the real world. We suspect this for two reasons.
656 First, storing information about non-optimal gaits seems valuable given that at times one may be
657 constrained from using the globally optimal gait. For example, the no-value function model
658 would need to relearn the optimal walking speed when constrained by a slow crowd that prevents
659 walking at the globally optimal speed. In contrast, the value function model, which has memory
660 of past non-optimal walking experience, could rapidly predict the new cost optimal speed in the
661 face of this constraint [54]. Ignoring this potentially useful past experience seems unlikely on the
662 part of the nervous system, given that there will be times when it is energetically beneficial to
663 recall it. Second, the simpler model avoids a value function only in the case where the learning
664 task has one dimension, such as in our experimental paradigm. If instead, for example, the
665 nervous system had to learn the optimal speed and step frequency it would need to store the
666 optimal step frequency, and its cost, at each speed. This is a one-dimensional value function for a
667 two-dimensional optimization problem. As the nervous system can't know a priori the
668 dimensionality of the optimization problem, it may benefit from learning a high dimensional
669 value function and then constraining the optimization problem depending on the constraints of
670 the task.

671 A simplified model that forgoes the updating of a reference cost prior to initiation of
672 optimization cannot reproduce key features of our experimental data. In our model of non-
673 spontaneous initiators, prior to initiation of optimization, the learner only updates a reference

674 cost (**Fig 1B**). Without this feature, direct and gradual convergence to the new energetic
675 optimum after forced experience with a low cost is not produced. Instead, because the reference
676 cost has not been updated and therefore is expected to be that experienced under the controller
677 off condition (Q^*_{off}), this model will first rapidly shoot back to the old cost optimum after
678 experience with a low cost. Only after updating this cost estimate, to its now higher cost value
679 under Q^*_{on} , will it then gradually adapt to the new optimum. This updating of a reference cost
680 prior to initiating optimization is not only necessary to reproduce our experimental findings, but
681 also has many parallels in neurophysiological habituation [13,52,53].

682 In all our models, we chose to discretize the possible actions, or step frequencies. This enforces
683 local learning, where actions at distinct step frequencies have no effect on the expected value of
684 others. It is entirely possible, if not likely, that the nervous system does not discretize its action
685 space in this way but may rather store a function. In other words, the value function may not be a
686 lookup table, as we have modeled it, but rather some representative equation, such as a
687 polynomial. However, it still seems likely that the nervous system updates its value function in
688 some localized way, as global function approximations are known to produce highly variable
689 behavior away from the local area of learning [55].

690 **ACKNOWLEDGMENTS**

691 This work was supported by a Vanier Canadian Graduate Scholarship (J.C.S.), a Michael Smith
692 Foundation for Health Research Fellowship (J.D.W.), the U.S. Army Research Office grant
693 #W911NF-13-1-0268 (J.M.D.), and an NSERC Discovery Grant (J.M.D.). We thank T.J. Carroll
694 and R.T. Roemmich for their helpful comments and suggestions.

695 **AUTHOR CONTRIBUTIONS**

696 J.C.S. and J.M.D. designed the study with input from J.D.W. and S.N.S.; J.C.S. collected data
697 and performed analysis; J.C.S. and J.M.D. wrote the manuscript. All authors discussed the results
698 and commented on the manuscript.

699 REFERENCES

- 700 1. Todorov E, Jordan MI. Optimal feedback control as a theory of motor coordination.
701 Nat Neurosci. 2002;5: 1226–1235. doi:10.1038/nn963
- 702 2. Todorov E. Optimality principles in sensorimotor control. Nat Neurosci. 2004;7:
703 907–915. doi:10.1038/nn1309
- 704 3. Scott SH, Norman KE. Computational approaches to motor control and their
705 potential role for interpreting motor dysfunction. Curr Opin Neurol. 2003;16: 693–
706 698. doi:10.1097/01.wco.0000102631.16692.71
- 707 4. Flash T, Hogan N. The coordination of arm movements: an experimentally
708 confirmed mathematical model. Journal of Neuroscience. 1985;5: 1688–1703.
- 709 5. Shadmehr R, Huang HJ, Ahmed AA. A Representation of Effort in Decision-
710 Making and Motor Control. Elsevier Ltd; 2016;: 1–7. doi:10.1016/j.cub.2016.05.065
- 711 6. Alexander RM. Optima for Animals. Princeton University Press; 1996.
- 712 7. Kuo AD, Donelan JM. Dynamic principles of gait and their clinical implications.
713 Phys Ther. American Physical Therapy Association; 2010;90: 157–174.
714 doi:10.2522/ptj.20090125
- 715 8. Srinivasan M, Ruina A. Computer optimization of a minimal biped model discovers
716 walking and running. Nature. 2005;439: 72–75. doi:10.1038/nature04113
- 717 9. Kording KP, Tenenbaum JB, Shadmehr R. The dynamics of memory as a
718 consequence of optimal adaptation to a changing body. Nat Neurosci. 2007;10: 779–
719 786. doi:10.1038/nn1901
- 720 10. Wolpert DM, Diedrichsen J, Flanagan JR. Principles of sensorimotor learning.
721 Nature reviews Neuroscience. Nature Publishing Group; 2011.: 1–13.
722 doi:10.1038/nrn3112
- 723 11. Bastian AJ. Understanding sensorimotor adaptation and learning for rehabilitation.
724 Curr Opin Neurol. 2008;21: 628–633. doi:10.1097/WCO.0b013e328315a293
- 725 12. Krakauer JW. Motor learning: its relevance to stroke recovery and
726 neurorehabilitation. Curr Opin Neurol. 2006;19: 84–90.
- 727 13. Shadmehr R, Krakauer JW. A computational neuroanatomy for motor control. Exp
728 Brain Res. 2008;185: 359–381. doi:10.1007/s00221-008-1280-5
- 729 14. Scott SH. Optimal feedback control and the neural basis of volitional motor control.
730 Nat Rev Neurosci. 2004;5: 532–546. doi:10.1038/nrn1427

- 731 15. Diedrichsen JR, Shadmehr R, Ivry RB. The coordination of movement: optimal
732 feedback control and beyond. *Trends Cogn Sci (Regul Ed)*. Elsevier Ltd; 2009;14:
733 1–9. doi:10.1016/j.tics.2009.11.004
- 734 16. Franklin DW, Wolpert DM. Computational mechanisms of sensorimotor control.
735 *Neuron*. 2011;72: 425–442. doi:10.1016/j.neuron.2011.10.006
- 736 17. Bernstein NA. The co-ordination and regulation of movements. 1967.
737 doi:10.1234/12345678
- 738 18. Bellman R. The Theory of Dynamic Programming. *Proceedings of the National*
739 *Academy of Sciences*. National Academy of Sciences; 1952;38: 716–719.
- 740 19. Sutton RS, Barto AG. *Reinforcement Learning*. MIT Press; 1998.
- 741 20. Wu HG, Miyamoto YR, Castro LNG, Ivezky BPO, Smith MA. Temporal structure
742 of motor variability is dynamically regulated and predicts motor learning ability.
743 *Nature Publishing Group*. Nature Publishing Group; 2014;: 1–13.
744 doi:10.1038/nm.3616
- 745 21. Tumer EC, Brainard MS. Performance variability enables adaptive plasticity of
746 “crystallized” adult birdsong. *Nature*. 2007;450: 1240–1244.
747 doi:10.1038/nature06390
- 748 22. Wilson RC, Geana A, White JM, Ludvig EA, Cohen JD. Humans use directed and
749 random exploration to solve the explore–exploit dilemma. *Journal of Experimental*
750 *Psychology: General*. 2014;143: 2074–2081. doi:10.1037/a0038199
- 751 23. Molen NH, Rozendal RH, Boon W. Graphic representation of the relationship
752 between oxygen-consumption and characteristics of normal gait of the human male.
753 *Proceedings of the Koninklijke ...*; 1971.
- 754 24. Elftman H. Biomechanics of muscle with particular application to studies of gait. *J*
755 *Bone Joint Surg Am*. 1966;48: 363–377.
- 756 25. Ralston HJ. Energy-speed relation and optimal speed during level walking. *Int Z*
757 *Angew Physiol*. 1958;17: 277–283.
- 758 26. Atzler E, Herbst R. *Arbeitsphysiologische Studien III*. *Pflugers Arch*. 1928;: 292.
- 759 27. Zarrugh MY, Todd FN, Ralston HJ. Optimization of energy expenditure during level
760 walking. *Eur J Appl Physiol Occup Physiol*. 1974;33: 293–306.
- 761 28. Umberger BR, Martin PE. Mechanical power and efficiency of level walking with
762 different stride rates. *Journal of Experimental Biology*. 2007;210: 3255–3265.
763 doi:10.1242/jeb.000950

- 764 29. Minetti AE, Capelli C, Zamparo P, di Prampero PE, Saibene F. Effects of stride
765 frequency on mechanical power and energy expenditure of walking. *Med Sci Sports*
766 *Exerc.* 1995;27: 1194–1202.
- 767 30. Donelan JM, Kram R, Kuo AD. Mechanical and metabolic determinants of the
768 preferred step width in human walking. *Proceedings of the Royal Society B:*
769 *Biological Sciences.* 2001;268: 1985–1992. doi:10.1098/rspb.2001.1761
- 770 31. Selinger JC, O'Connor SM, Wong JD, Donelan JM. Humans Can Continuously
771 Optimize Energetic Cost during Walking. *Current Biology.* Elsevier Ltd; 2015;25:
772 2452–2456. doi:10.1016/j.cub.2015.08.016
- 773 32. Wolpert DM, Ghahramani Z. Computational principles of movement neuroscience.
774 *Nat Neurosci.* Nature Publishing Group; 2000;3: 1212–1217.
- 775 33. Scott SH. Optimal feedback control and the neural basis of volitional motor control.
776 *Nat Rev Neurosci.* 2004;5: 532–546. doi:10.1038/nrn1427
- 777 34. Krakauer JW, Mazzoni P. Human sensorimotor learning: adaptation, skill, and
778 beyond. *Current Opinion in Neurobiology.* 2011;21: 636–644.
779 doi:10.1016/j.conb.2011.06.012
- 780 35. Pagliara R, Snaterse M, Donelan JM. Fast and slow processes underlie the selection
781 of both step frequency and walking speed. *Journal of Experimental Biology.* The
782 *Company of Biologists Ltd;* 2014;217: 2939–2946. doi:10.1242/jeb.105270
- 783 36. O'Connor SM, Donelan JM. Fast visual prediction and slow optimization of
784 preferred walking speed. *Journal of Neurophysiology.* 2012;107: 2549–2559.
785 doi:10.1152/jn.00866.2011
- 786 37. Verkerke GJ, Hof AL, Zijlstra W, Ament W, Rakhorst G. Determining the centre of
787 pressure during walking and running using an instrumented treadmill. *Journal of*
788 *Biomechanics.* 2005;38: 1881–1885. doi:10.1016/j.jbiomech.2004.08.015
- 789 38. Sutton RS, Barto AG, Systems RWIC, 1992. Reinforcement learning is direct
790 adaptive optimal control. *ieeexploreiee.org.*
- 791 39. Collins S, Ruina A, Tedrake R, Wisse M. Efficient bipedal robots based on passive-
792 dynamic walkers. *Science.* 2005;307: 1082–1085. doi:10.1126/science.1107799
- 793 40. Peters J, Schaal S. Reinforcement learning of motor skills with policy gradients.
794 *Neural Networks.* 2008;21: 682–697. doi:10.1016/j.neunet.2008.02.003
- 795 41. Lillicrap TP, Hunt JJ, Pritzel A, Heess N, Erez T, Tassa Y, et al. continuous control
796 with deep reinforcement learning. 2015.
- 797 42. Schultz W, Dayan P, Science PM, 1997. A neural substrate of prediction and
798 reward. *sciencesciencemag.org*

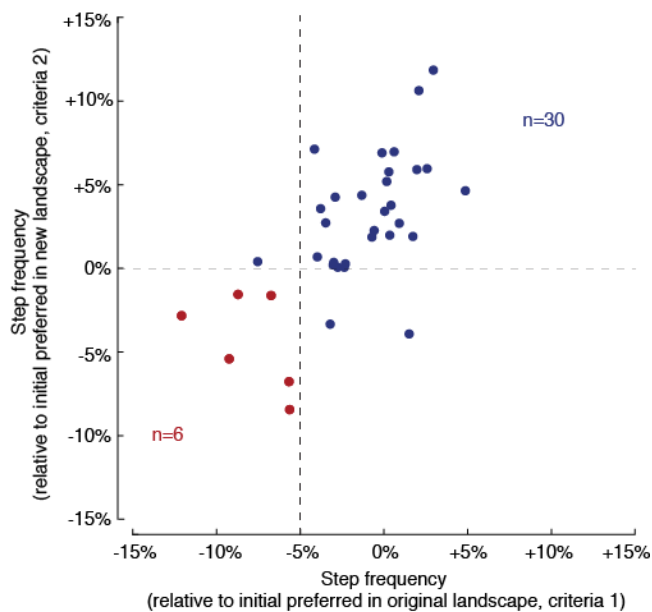
- 799 .
- 800 43. Adams JA. A Closed-Loop Theory of Motor Learning. *J Mot Behav*. 2nd ed.
801 Routledge; 1971;3: 111–150. doi:10.1080/00222895.1971.10734898
- 802 44. Adams JA. Issues for a Closed-Loop Theory of Motor Learning. Elsevier
803 . Elsevier; 1976;: 87–107. doi:10.1016/B978-0-12-665950-4.50009-2
- 804 45. Wolpert DM, Miall RC. Forward Models for Physiological Motor Control. *Neural*
805 *Netw*. 1996;9: 1265–1279.
- 806 46. Wolpert DM, Landy MS. Motor control is decision-making. *Current Opinion in*
807 *Neurobiology*. Elsevier Ltd; 2012;22: 996–1003. doi:10.1016/j.conb.2012.05.003
- 808 47. Wolpert DM, Ghahramani Z, Flanagan JR. Perspectives and problems in motor
809 learning. *Trends Cogn Sci (Regul Ed)*. 2001;5: 487–494.
- 810 48. Wu HG, Miyamoto YR, Gonzalez Castro LN, Ölveczky BP, Smith MA. Temporal
811 structure of motor variability is dynamically regulated and predicts motor learning
812 ability. *Nature Publishing Group*. 2014;17: 312–321. doi:10.1038/nm.3616
- 813 49. Herzfeld DJ, Shadmehr R. Motor variability is not noise, but grist for the learning
814 mill. *Nature Publishing Group*. *Nature Publishing Group*; 2014;17: 149–150.
815 doi:10.1038/nm.3633
- 816 50. Scholz JP, Schöner G. The uncontrolled manifold concept: identifying control
817 variables for a functional task. *Exp Brain Res*. 1999;126: 289–306.
- 818 51. Reinkensmeyer D, Aoyagi D, Emken J, Galvez J, Ichinose W, Kerdanyan G, et al.
819 Robotic gait training: toward more natural movements and optimal training
820 algorithms. *Conf Proc IEEE Eng Med Biol Soc*. 2004;7: 4818–4821.
821 doi:10.1109/IEMBS.2004.1404333
- 822 52. Desmurget M, Grafton S. Forward modeling allows feedback control for fast
823 reaching movements. *Trends Cogn Sci (Regul Ed)*. 2000;4: 423–431.
- 824 53. Wolpert DM. Computational approaches to motor control. *Trends Cogn Sci (Regul*
825 *Ed)*. Elsevier; 1997;1: 209–216. doi:10.1016/S1364-6613(97)01070-X
- 826 54. Snaterse M, Ton R, Kuo AD, Donelan JM. Distinct fast and slow processes
827 contribute to the selection of preferred step frequency during human walking. *J Appl*
828 *Physiol*. 2011;110: 1682–1690. doi:10.1152/jappphysiol.00536.2010
- 829 55. Atkeson CG, Moore AW, learning SSL, 1997. Locally weighted learning for
830 control. Springer.
- 831

832 **SUPPORTING INFORMATION CAPTIONS**

833 **Table S1. Subject numbers per experiment.** We initially tested 9 subjects in each of the three
 834 Second Experience testing periods. To account for a high number of spontaneous initiators in the
 835 self-guided broad experience condition we added an additional 2 subjects to this group to
 836 rebalance our conditions. To achieve the statistical power necessary to investigate the interaction
 837 between high and low cost experience, as well as the order of the experience, we added an
 838 additional 7 subjects to the metronome-guided discrete experience experiment, one of which we
 839 found to be a non-spontaneous initiator. In total, we tested 36 subjects, 6 of which were
 840 classified as spontaneous initiators and 30 which were non-spontaneous initiators.

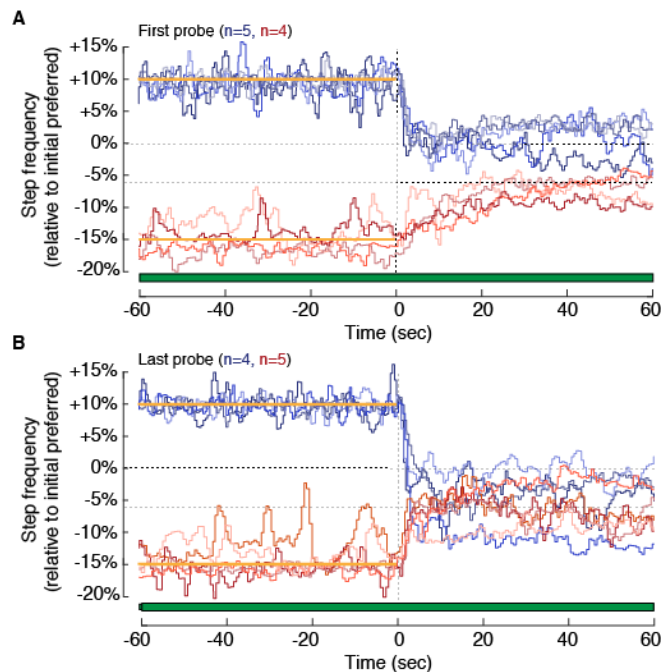
Second experience	Initial subjects		Added to rebalance		Added to explore high low		Total subjects		
	Spont.	Non-Spont.	Spont.	Non-Spont.	Spont.	Non-Spont.	Spont.	Non-Spont.	All
Metronome-guided discreet	1	8	0	0	1	6	2	14	16
Metronome-guided broad	1	8	0	0	0	0	1	8	9
Self-guided broad	3	6	0	2	0	0	3	8	11
Total	5	22	0	2	1	6	6	30	36

841



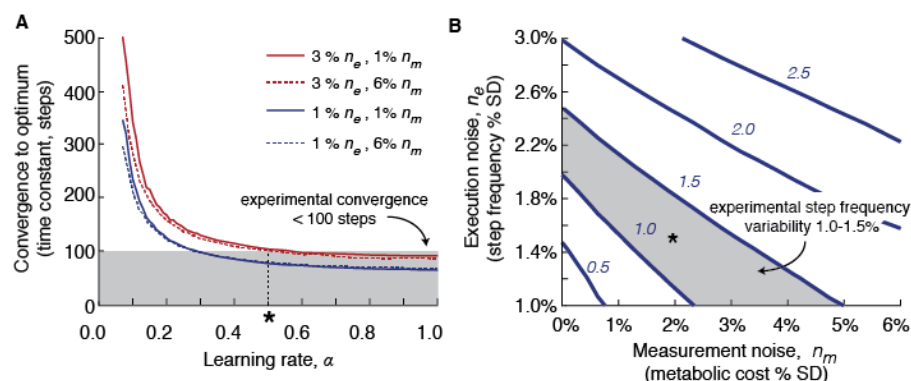
842

843 **Fig S1. Discrimination plot of spontaneous and non-spontaneous initiators.** We defined
 844 spontaneous initiators as having a first experience final step frequency consistent with the
 845 expected optima (-3SD from the initial preferred step frequency, or approximately -5%, x-axis),
 846 as well as displaying a significant change in step frequency from that displayed immediately
 847 after the exoskeleton was turned on (significantly different from 0%, y label). Although the
 848 above statistics, and not simple thresholds, were used for each criteria, the dashed lines illustrate
 849 roughly how each criteria divided the data.



850

851 **Fig S2. Individual subject effect of experience direction during first and last step frequency**
 852 **probe.** Step frequency time-series data for the first (A) and last (B) probes following experience
 853 either high (blue) or low (red) step frequencies for individual subjects. The horizontal bars
 854 indicate when the controller is turned on (green fill) and off (white fill), and the yellow lines
 855 indicate the prescribed metronome frequencies.



856

857 **Fig S3. Sensitivity analysis of model parameters.** (A) Effect of varying the learning rate
 858 parameter on the rate of converge to the energetic optimum for different measurement and
 859 execution noise levels. The shaded region represents a reasonable convergence rate given that
 860 observed experimentally (maximum 100 steps), while the asterisk and dashed vertical line
 861 represents the chosen learning rate parameter value used in simulation (0.5). (B) Effect of
 862 varying measurement and execution noise on variability in steady state step frequency. Learning
 863 rate was kept constant at 0.5. Each line and the associated italic number represents a constant
 864 value of steady state step frequency. The shaded region represents reasonable steady state step

865 frequencies given that observed experimentally (1.0%-1.5%). The asterisk represents the chosen
866 measurement and execution noise parameter values used in simulation (2.0% and 1.5%,
867 respectively).